SLAC – PUB – 4578
August 1988
(E/I)

The Mark III Vertex Chamber†

J. Adler,[1] T. Bolton,[1] K. Bunnell,[2] R. Cassell,[2] E. Cheu,[3] R. Eisele,[2] T. Freese,[4] C. Grab,[2] G. Mazaheri,[2] R. Mir,[5] A. Odian,[2] D. Pitman,[2] W. Stockhausen,[6] W. Toki,[2] F. Villa,[2] W. Wadley,[2] S. Wasserbaech,[2] W. Wisniewski[7]

Stanford Linear Accelerator Center, Stanford, CA 94309

Abstract

We have constructed and installed a pressurized straw vertex chamber in the Mark III experiment at the SLAC e^+e^- storage ring SPEAR. The chamber consists of 12 concentric layers of straws, arrayed at radii between 5.4 cm and 13.0 cm from the interaction point. There are a total of 640 straws, each 8 mm in diameter and 84 cm long. We obtain an overall spatial resolution of 49 μm for argon-ethane (50%/50%) at 3 atmospheres absolute using a cosmic ray data sample. The effects of gases on various chamber materials have been investigated. Chamber lifetime studies have been performed. A prototype chamber was used to study the resolution obtained with various gases.

Submitted to *Nuclear Instruments and Methods B*

1 Massachusetts Institute of Technology, Cambridge, MA 02138.
2 Stanford Linear Accelerator Center, P.O. Box 4349, Stanford, CA 94309.
3 Present address: Cornell University, Ithaca, N.Y. 14853.
4 University of Illinois at Urbana-Champaign, Urbana, IL 61801.
5 University of Washington, Seattle, WA 98195.
6 Present address: Bayer AG, Leverkusen, D-5090 Bayerwerk, West Germany.
7 California Institute of Technology, Pasadena, CA 91125.

† This work was supported in part by the Department of Energy, under contracts DE-AC03-76SF00515, DE-AC02-76ER01195, DE-AC03-81ER40050, DE-AM03-76SF0034, and by the National Science Foundation.

1. Introduction

Several experiments[1-3] have demonstrated the feasibility and utility of high resolution inner drift chambers constructed of aluminized Mylar straws. In particular, one such chamber has been used at the e^+e^- storage ring PEP to measure the average lifetime of B mesons.[2] These chambers consist of many tubes, or *straws,* mounted parallel to the beam direction, with anode wires running along the axis of each straw. They offer the advantages of a robust electrical and mechanical design, ease of construction, and modest cost, without sacrificing performance. The closed-cell design of the chamber eliminates problems such as photon feedback and neighbouring channel crosstalk. In addition, the modularity allows for individual channels to be disconnected. Spatial resolutions of less than 50 μm can be achieved.

The Mark III experiment, operating at the SLAC e^+e^- storage ring SPEAR, has been recently outfitted with a twelve-layer pressurized straw-type vertex chamber. At SPEAR center-of-mass energies (3-7 GeV), the uses of the chamber will be multifold. The low-radiation length vertex detector provides a primary trigger for the Mark III detector, replacing the original trigger chamber. By including radial and longitudinal spatial information at small radii, the solid angle acceptance for tracking charged particles can be increased from 85% to 95% of 4π steradians. This should enhance particle identification in that decaying kaons may be tracked and identified by their kink topology. The increased angular acceptance should produce a major improvement in detection efficiencies for the reconstruction of exclusive multi-body final states, such as $e^+e^- \rightarrow D_s^+D_s^- \rightarrow (\phi\pi)(\eta\pi) \rightarrow K^+K^-\pi^+\pi^+\pi^-\pi^-\pi^0$. The larger solid an-

gle coverage enhances the capabilities for spin-parity analyses of states such as the $\eta(1440)$, produced in $e^+e^- \rightarrow J/\psi \rightarrow \gamma\eta(1440)$ with a production angle distribution peaked at small angles. Several interesting final states, such as $e^+e^- \rightarrow D^{*+}X$, $D^{*+} \rightarrow \pi^+D^0$, require the detection of slow pions. Such tracks can be measured completely using information from the new vertex chamber alone. Finally, the vertex detector will allow very clean identification of detached vertices in K^0_S and Λ decays, which will improve background rejection capabilities in final states containing these particles. A Monte Carlo simulation showed that detached charmed particle vertices of 200 μm in the transverse plane could be detected for center-of-mass energies of 5-6 GeV, assuming 50 μm spatial resolution for the chamber.

The chamber was built and tested in approximately three months. It was installed in the detector in the west interaction region of SPEAR in the summer of 1987. A cosmic ray data run followed, during which 8×10^5 events were collected.

The design and construction of the chamber are described in Section 2. The beam pipe and its related structure are described in Section 3. The construction details are discussed in Section 4. The gas system is described in Section 5 and the readout and electronics in Section 6. Section 7, 8, and 9 discuss the results of prototype tests, studies of drift chamber materials, and studies of the chamber lifetime. The results of the cosmic ray run are given in Section 10. Section 11 describes how the vertex chamber is used in the event trigger. Conclusions appear in Section 12.

2. Chamber Design

The chamber, depicted in Figure 1, consists of 640 aluminized Mylar[4] drift tubes arranged in eight concentric axial layers and four stereo layers. The innermost layer is at a radius of 5.4 cm, the outermost layer at 13.0 cm. The straws are 8 mm in diameter and are fixed at each end to the *inner* endplates. The endplates, made of 2.54 cm thick aluminum, are separated by 84 cm and epoxied to the beam pipe. A second set of 2.54 cm thick aluminum endplates, the *outer* endplates, is clamped to the beampipe. A 0.75 mm thick graphite-fibre cylindrical shell is fixed to the outer endplates. The shell, the outer endplates, and the beam pipe form the pressure vessel. The readout cables pass through the outer endplates. The vessel allows operation of the chamber at pressures of up to 4 atmospheres absolute.

The arrangement of the straws, shown in Figure 2 and described in Table 1, was chosen to optimize the number of axial hits per track. Layers one through four are axial layers with 40 straws in each layer. In contrast to previous straw chambers, successive layers are offset by 1/4 cell. Layers five through eight are stereo layers with 40 straws in each. Layers nine through twelve are axial layers with 80 straws in each layer, offset in the same pattern as layers one through four. Thus, tracks which pass near the sense wire in one layer will pass midway between the sense wire and the tube wall in the successive layer. This ensures that each track will have at least two high resolution measurements in each group of four layers. The maximum drift distance in each cell of 4 mm corresponds to a drift time of 80 ns for argon-ethane.[5]

Layer	ϕ of wire 1 (radians)	Radius at $z = 0$ (cm)	Stereo angle (degrees)
1	$\frac{\pi}{40}$	5.42	0
2	$\frac{\pi}{20}$	6.09	0
3	$\frac{\pi}{80}$	6.85	0
4	$\frac{3\pi}{80}$	7.43	0
5	$\frac{3\pi}{80}$	8.23	3.000
6	$\frac{5\pi}{80}$	8.70	3.168
7	$\frac{\pi}{80}$	9.50	−3.460
8	$\frac{3\pi}{80}$	9.78	−3.561
9	$\frac{\pi}{40}$	10.92	0
10	$\frac{3\pi}{80}$	11.60	0
11	$\frac{3\pi}{160}$	12.36	0
12	$\frac{5\pi}{160}$	13.00	0

3. Beam Pipe and Pressure Vessel

To minimize multiple Coulomb scattering and photon conversion, the vertex detector was constructed directly on a beryllium beam pipe. The central 41 cm portion of the beam pipe, made of 1.27 mm thick beryllium, has an outer diameter of 9.78 cm. It is brazed to an aluminum segment of thickness 0.32 cm and with a 10.03 cm outer diameter.

Given the smaller diameter and thickness of the new beryllium beam pipe, it was necessary to take several steps to minimize synchrotron radiation background. Data from previous running periods showed that this background appeared to be due to backscattering in the stainless steel beam pipe at the ends of the Mark III detector. A lead mask, external to the beam pipe, was added at each end of the beam pipe assembly roughly 1 meter from the interaction point.

The mask has an average thickness of 7.3 cm and has an inner and outer radius of 4.1 cm and 9.2 cm respectively. The remainder of the beam pipe was made of aluminum rather than stainless steel, which reduces the energy of the fluorescent photons to 1.5 keV, due to the lower K-edge of aluminum. These lower energy photons are more likely to be absorbed outside of the detector region. To further aid in the absorption of photons, the beryllium segment of the beam pipe was plated with a 15 μm thick layer of nickel on the inside, and a 25 μm thick titanium foil was placed between the beam pipe and the first layer of straws.

The shell of the pressure vessel[6] was made of a graphite fibre/epoxy laminate chosen for its strength and low density. It was constructed by winding the graphite fibres, 75 μm in diameter, on a mandrel and impregnating these with epoxy. A 50 μm Kapton[7] liner was glued to the inside of the shell to act as a gas seal. The vessel was successfully tested to 4 atmospheres absolute. Following the construction of the chamber, the shell was slid into place and clamped to the endplates with an O-ring seal. (A temporary steel vessel was used to test the vertex chamber during its construction.) A 50 μm layer of aluminum was placed on the outer surface of the vessel and attached to the outer endplates. This should provide a continous path for currents on the outer surface of the beam pipe, which would otherwise flow through the vertex detector.

Preliminary studies of synchrotron radiation background have been made with electrons in the SPEAR ring. With a beam energy of 2.355 GeV and a current of 5 mA, measurements were made for a sample of wires. The chamber was operated at a pressure of 3 atmospheres absolute, with a sense wire voltage of 3.9 kV. The inner two axial layers drew approximately 1.5 μA (total) and

had singles rates of approximately 400 Hz per tube, for nominal pulse height thresholds corresponding to 0.36 mV at the input of the amplifier. Layers 11 and 12 drew 0.5 μA and had singles rates of 60 Hz/tube. To scale to typical running conditions for center-of-mass energies of 4.7 GeV, there are additional factors of 2 (due to two beams) and of ≈ 5 due to the increased beam currents. Typical SPEAR beam currents range from 3-4 mA per beam for center-of-mass energies of 3 GeV, to 20-25 mA per beam at 6 GeV.

The components of the detector are listed in Table 2.

Component	Diameter (cm)	Thickness (mm)	Length (cm)	X/X_0 (%)
Beryllium beampipe	9.53	1.27	40.64	0.36
Nickel plating	9.53	0.0157	40.64	0.103
Titanium foil	9.78	0.0254	40.62	0.071
Straws	0.78 ea	0.100	83.82	0.925 ea
Wires	0.005 ea	-	83.82	0.0616 ea
Pressure Vessel Can	27.08	0.8	144.78	0.196
Kapton liner	27.07	0.051	134.62	0.018
Aluminum cover	27.23	0.051	150	0.057
argon-ethane (3 atm)	-	-	-	0.165

4. Construction details

The requirements of high precision which depends upon good mechanical tolerances and minimal channel-to-channel crosstalk dictated the design for the mounting of the straws. While sufficient tension on the straw ensures the straightness of the straw and hence the certainty of the wire position, maintaining a coaxial system without interruption was found to be paramount to minimizing

crosstalk problems. In this chamber, the straws have been mounted such that they are under tension and the ends are flush against the endplates.

The straws[8] are constructed of two layers of Mylar, 25 μm and 50 μm thick, each coated on one side with a film of aluminum $0.25-0.30$ μm in thickness. The layers are helically wound and laminated so that the aluminum film forms the inner and outer surfaces of the straw. The resulting straws are 100 μm thick and have an end-to-end surface resistance of about 15Ω. The straws were selected for straightness, electrical continuity, surface quality, and general resilience. Three of the straws have been painted on the outer surface with a radioactive paint containing ^{55}Fe, providing well-defined (rate $\approx$ 100 Hz) signal pulses for debugging purposes.

At each end of the straw is a Delrin[9] feedthrough (Figure 3), through which the sense wire passes. The feedthroughs, based on a design used in the MAC chamber,[2] are held in place by aluminum rings which are glued to the straw using silver-loaded epoxy.[10] The feedthroughs fit tightly into the holes in the endplates and are slotted to allow gas to flow into the straws.

The straws were tensioned to 500 g by preparing them such that they were 0.6 mm shorter than the distance between the endplates, and then stretching them until they touched the endplates. The aluminum rings sit flush against the endplates (Figure 3) and it is this contact which forms the electrical ground. The stereo holes are counter-bored to allow the ends of the straws to lie flat against the surface of the endplate.

The sense wire is 50 μm diameter gold-plated tungsten tensioned to 275 g.

The wire passes through stainless steel pins which are press-fitted into holes in the center of the feedthroughs. The pins, which have an inner diameter of 115 μm and outer diameter of 990 μm, are crimped to hold the wire.

Several factors contribute to the accuracy of the wire positions: the location of the wires within the pins, the location of the holes in the inner endplates, and the electrostatic deflection of the wires. The precision with which the chamber is assembled is reflected in all of the above.

The coordinates of all the holes in the inner endplates were measured to an accuracy of 10 μm.[11] The holes have a diameter of 4.22 mm. The axial holes, drilled with a numerically-controlled mill, are within 50 μm of their design locations. The stereo holes, drilled with a hand-controlled Bridgeport mill, are within 125 μm of the design locations. We estimate the error in the wire position to be ± 25 μm at the endplates, due to the uncertainty of the wire position in the stainless steel pins.

Two problems can contribute to an electrostatic deflection of the sense wire: the wire is initially off-center (for instance, due to the feedthrough positions) or the straw has a curvature. An initial displacement δ of the 50 μm diameter sense wire will lead to a deflection of $\approx 0.08\ \delta$ due to the electrostatic deflection, for voltages of 4 kV. For the case of the curved straw, the deflection of the wire is $\approx 6\%$ of the straw sagitta, for voltages of 4 kV. The straws were rotated such that any possible bowing was in the radial direction, where it will have a negligible impact on the momentum measurement, and the spacing between straws in a given layer was made uniform. The typical variation in straw spacing of 0.1 mm would cause an azimuthal wire deflection of 6 μm which contributes directly to

the momentum measurement. The resulting total error in the wire position is a limiting factor on the spatial resolution which can be achieved.

The entire length of the wires and cables is shielded to prevent crosstalk. One end of each wire is connected to a high voltage/signal cable. The connectors, designed and manufactured at SLAC, consist of a socket which fits on the pin, an insulating Delrin collar attached to the feedthrough, and a brass collar soldered to the end of the cable braid. The brass collar makes electrical contact with the endplate, as shown in Figure 3. The pin at the opposite end of the sense wire is shielded by a 4 cm long Delrin-insulated brass collar.

Because compact, pressure- and high voltage-rated connectors for the outer endplates were not commercially available, the HV cables were glued into the outer endplates. A one cm thick layer of Stycast[12] epoxy was poured onto the endplate and pressurized to 4 atmospheres absolute. After gluing, a leak rate of 0.004 l/minute (STP) per endplate was observed at 4 atmospheres absolute pressure. Following the handling of the endplates and the cables over the period of several months, the leak rate of the chamber has increased to 0.8 l/minute, for pressures of 4 atmospheres absolute. Most of the leak rate occurs through the cables.

The chamber was assembled and tested one layer at a time. The electrical conductivity between the straw surfaces and the endplates was checked. Wire tensions were monitored by measuring the resonant vibration frequency of the wire in a magnetic field. The tension was required to be within 13% of the nominal value. After each layer was completed, the chamber was placed in a temporary pressure vessel and filled with argon-ethane gas. An ^{55}Fe source,

plated on a thin meter-long strip of copper,[13] was wrapped around the layer of straws in a belt-like fashion and each straw was checked for pulse height and crosstalk. Anomalously large pulse heights usually indicated that the sense wire was off-center or that the straw was excessively bowed. Those channels which failed any of the tests had the straws or sense wires replaced as necessary.

5. Gas system

The gas system consists of the chamber, the gas supply, the electropolished stainless steel pipes, a pressure regulator, and a mixer. The chamber holds a gas volume of approximately 70 l. No silicon-based products have been used. Black Viton[14] O-rings have been used at the joints between the outer endplates and the pressure vessel. Only analysed 50% argon 50% ethane gas is used for chamber operation.

A Datametrics[15] 1501 control system in conjunction with a Barocel 590 A pressure transducer and a Brooks[16] 5835 servo valve controls the pressure. The device is accurate to 0.007 bar, with a stability of $\approx$ 0.007 bar over a six-month period. The temperature is monitored by four thermocouples, Analog Devices[17] AD590JF, mounted inside the detector near the inner and outer radii of each outer endplate. Temperature variations are expected to change the drift velocity (in argon-ethane) by less than 2% over the course of the running period.

6. Electronics and Readout

The vertex chamber electronics system consists of a high voltage power supply, a high voltage distribution/display box, high voltage board, the amplifier-discriminator card, a threshold control module, a threshold card, the time-to-

analog-converter module (TAC2) readout system, the time readout control module, and the calibration system.

The high voltage is supplied by a Bertan[18] 1755P module and distributed through a custom-made high voltage distribution/display box via RG-59 cables to 40 high voltage boards. Each board has 16 channels, covering 16 adjacent wires in two layers. A schematic of the HV system is shown in Figure 4. In each channel, the sense wire is connected to high voltage through a 22 MΩ resistor and an RG 122/4 cable.[19] A 680 pf capacitor couples the sense wire to the signal cable (32 ns RG 174). The high voltage system has been designed for maximum operating voltages of 5 kV.

The amplifier/discriminator module has 16 channels/board. The amplifier, based on an Avantek[20] MSA-0135-22-RF, has been designed to accommodate several configurations so that the gain, bandwidth, impulse response, and input impedance may be easily changed. It may be operated in a two-stage configuration (gain ≈ 60) or in a three-stage configuration (gain ≈ 700); we have chosen the former. The bandwidth response is shown in Figure 5. For the two-stage case, it ranges from 100 kHz to 500 MHz. The amplifier has a risetime of 1.5 ns, (shown in Figure 6), input noise 5.6 dB above thermal noise, and low crosstalk. The noise counting rate is shown in Figure 7. From threshold settings we estimate the gain at which the chamber is typically operated to be a few 10^5 for single electrons; for minimum ionizing particles the gain is measured to be $\approx 6 \times 10^4$, corresponding to pulse heights of ≈ 2 mV, before amplification. The apparent lower gain for minimum ionizing particles may be due to saturation of the gain in the presence of many electrons. The discriminator is based on the LeCroy[21]

MVL407 chip and the discriminator level for each board can be remotely controlled on an individual basis. The threshold setting used corresponds to about one electron charge on the sense wire.

The TAC2 modules[22] were modified to provide stable and low noise operation at a full range of 300 ns. This was done by lowering the ramp and range voltages, and by capacitively suppressing the noise level on the boards. Separate high-precision power supplies (Power Design[23] model 5020) are connected through thick copper cables to reinforced backplane bars to keep the voltages on both the load and ramp capacitors stable to better than 2 mV.

A control module generates the reference signals for the drift time measurements in the TAC2's. A BADC module[24] is used to serially read out the analog data and perform quadratic corrections to the drift times before the data are read out via CAMAC to a VAX computer.

The system is calibrated by use of a separate control module, which generates well defined calibration pulses through capacitive coupling on the HV boards.

7. Cosmic Ray Results

Following the installation of the vertex chamber in the interaction region, 8×10^5 cosmic ray events were recorded with the chamber. The chamber was operated at 3 atmospheres absolute and 3.9 kV. This allowed a full test of the performance and alignment of the vertex chamber, though without the use of a magnetic field. The events were iteratively fitted by the procedure described below. Figure 8 shows the results of the fit for a typical event.

Six parameters describe a given channel, i: t_{0i} (channel start times), $v_i(r)$

(the time-to-distance relationship), x_i and y_i (the position of the center of the wire at the south endplate), $\frac{\partial x_i}{\partial z}$ and $\frac{\partial y_i}{\partial z}$.[25] For the first iteration, the survey wire positions and a measured time-to-distance curve common to all wires were used. The axial hits in each event were fitted to a straight line in space. Two parameters describe the track: x_0 is the x value where the track intersects the plane $y = 0$, and $\frac{\partial x}{\partial y}$ is the slope in the xy-plane. A drift distance for each wire hit was calculated. After making corrections for the transit time along the length of the wire of the pulse, run-by-run t_{0i}, and z position of the hit, the residual for each wire, defined as the fitted distance of the track from the wire minus the drift distance, was determined. The fit minimizes the sum of the squares of the residuals divided by the number of hits for each event.

The results of the fit were used to survey the chamber. The x and y components of the residuals for channel i were plotted vs. z and fitted to a straight line to obtain x_i, y_i, $\frac{\partial x_i}{\partial z}$ and $\frac{\partial y_i}{\partial z}$. The residuals were fitted vs. t for each channel, to obtain t_{0i} and $v_i(r)$. Using the fitted parameters as input, the fit was repeated until it converged.

The distribution of the residuals for all channels is shown in Figure 9. The overall resolution, defined as the sigma of this distribution, is 49 μm for tracks at all radial distances. The single-wire resolution from the fit varies between 40 and 70 μm. Figure 10 shows the resolution as a function of the radial distance from the wire.

8. Prototype Tests

A prototype containing 6 straws was used to measure the resolution and gain

in various gases.[26] The gases used were argon-ethane, argon-ethane with 0.2% water vapour, and dimethyl ether (DME). The straws were identical to those of the chamber and were arranged in vertical triplets, the center straw offset horizontally by 180 μm.

Figure 11a shows the single tube resolution vs. $\frac{V}{P}$ in argon-ethane. Data were taken at pressures of 1, 2, 3 and 4 atmospheres absolute. The single wire resolution achieved at 2, 3, and 4 atmospheres is better than 40 μm. The expected dependence of the resolution, $\sigma \propto P^{-1/2}$, is evident. The addition of 0.2% water to the argon-ethane did not significantly change the resolution.

The resolution vs. $\frac{V}{P}$ for DME at one atmosphere absolute is shown in Figure 11b. A resolution slightly better than 40 μm was obtained over a wide range of operating voltages at this pressure. The data includes tracks at all radial and longitudinal positions in the tubes. No corrections have been made for the longitudinal position of the track.

9. Materials Studies

Two sets of tests were made to study the effects of pressurized gases on various drift chamber materials. Straws and sheets of aluminized Mylar were sealed for a one-month period in pipes filled with the following gas mixtures: pressurized air (to check the effect of pressure alone), DME, argon-ethane, and argon-ethane with water. The results of the test are shown in Figure 12. Those straws exposed to DME increased in weight by 2.5% and in length by 0.35%. The aluminized Mylar sheet showed a tendency to curl along its length and the Delrin feedthroughs swelled. In no other gas was there a measurable effect on

the samples.

In the second set of tests, samples of G-10,[27] Kapton, Stesalit,[28] Celanese X,[29] Delrin, and aluminized Mylar straws were left for a one-month period in vessels containing DME and argon-ethane with 0.5% ethanol. The results of the test are shown in Figure 13. Though the data are by no means complete, they indicate that DME has a substantial effect on Kapton, Delrin, and aluminized Mylar. The relative change in weight of these samples is $\approx 10^{-2}$. The argon-ethane with ethanol had a similar effect on the Kapton. The changes in the Kapton may, however, have been simply due to its hygroscopic nature. In addition, the argon-ethane with ethanol showed a marginal effect on the Mylar straws amounting to a relative change in weight of $\approx 4 \times 10^{-3}$.

10. Chamber Lifetime Studies

Since the aging process of drift chambers in high radiation environments is not well-understood, studies were made to prolong the lifetime of a test chamber. We expect that the vertex chamber would be exposed to ≈ 0.01 C/cm of radiation per normal annual operation in the SPEAR ring. Of the gas additives (water and various alcohols) referred to in the literature,[30] water was found to be the most benign vis-à-vis the Mylar straws. The effects of small admixtures of water vapour to the argon-ethane gas mixture and rate of gas flow were therefore investigated.

The test apparatus consisted of four straws, surrounded with an ^{55}Fe source etched on a thin copper sheet, which uniformly irradiated each straw over a length of 10 cm. Data were taken at 3 atmospheres absolute pressure and 3.9 kV. This

typically furnished a singles rate of $\approx$ 100 kHz per tube and a current of $\approx 3\ \mu$A per tube as the initial operating conditions. The straw lifetime, measured in C/cm, was presumed to be terminated when the current and singles rate began to escalate. This usually occurred after several days of operation during which the current and the singles rate had been for the most part constant.

The lifetime of a cell, without frequent gas circulation or the addition of water vapour, was $\approx$ 0.02 C/cm. By changing the argon-ethane in the straws approximately every 100 s, the lifetime of a cell was prolonged by greater than a factor of $\approx$ 3, as shown in Table 3. The addition of a small percentage of water to the gas mixture was beneficial only under conditions of frequent gas flow, where an increase by a factor of $\approx$ 10 was observed in the lifetime of the test chamber. The amount of water which may be added, however, is limited at normal operating temperatures to $\approx$ 0.2% because of condensation in the chamber.

Water Vapor (%)	Chamber Lifetime (C/cm) No Gas Flow	Chamber Lifetime (C/cm) With Gas Flow
0.0	0.027±.002	0.07±.01
0.2	0.026±.003	> 1.0
0.4	0.022±.002	> 0.8

11. Trigger

A major benefit provided by the vertex chamber is the enhancement of the capabilities of the Mark III event trigger. The Mark III trigger[31] has two levels. In the first, a preliminary decision on event viability is made within 600 ns of

beam crossing (which occurs every 781 ns), allowing sufficient time to reset the detector electronics. In the second, the main drift chamber data is used to track charged particles and to make the final event trigger decision. The goal of the trigger upgrade is the reduction of the first level trigger rate at high energy, while maintaining maximum efficiency and compatibility with the second level trigger. The high granularity afforded by the vertex chamber and the short maximum drift time, 80 ns, permit a fast first level decision. The ability to require multiple coincidences is then used to reduce the first level rate at high energies, where the intensity of synchrotron radiation would otherwise cause high trigger rates.

The trigger is based on finding track segments in the "r $-$ ϕ" plane. Track segments are formed by associating sets of tubes, called *elements,* in the inner four axial layers with elements from the outer four axial layers. The definition of an element and the choice of logical combination of elements are software selectable and can be adapted to the running environment. Elements are defined as follows: the signal from each tube in layers 1 and 2 is combined (AND/OR) with the logical OR of the signals from the two subtended adjacent tubes in layers 3 and 4 (shown in Figures 15a and b). The AND/OR choice depends on the background accidental rate, which is a function of the beam energy. The outer axial layers are treated analogously.

The first level trigger is formed by combining elements from inner layers with the three subtended elements from the outer layers. This combination allows for curvature of charged tracks in the magnetic field. Using the measured singles rate per tube obtained in beam tests, 400 Hz, the extrapolated first level trigger rate due to synchrotron radiation accidentals is less than 1 Hz when the tightest

logic conditions are imposed. Since rates up to 10 kHz can be tolerated, there is considerable latitude in trigger condition selection.

In order to remain compatible with the second level trigger, 32 signals must be generated from the vertex chamber to match the segmentation in ϕ of the main drift chamber. To accomplish this, the signals from the 160 outer elements are ORed in groups of five and are passed on to the second level trigger.

The scheme described above allows considerable flexibility by permitting maximization of efficiency at low energy, where requirements can be lax, and optimization of beam related background rejection at high energy, where more severe topological constraints can be applied.

12. Conclusions

We have constructed and installed a 12-layer straw vertex chamber for use in the Mark III experiment. The chamber will provide increased angular acceptance for tracking low-momentum and decaying particles and will be used in the first-level event trigger. An overall spatial resolution of 49 μm was achieved using a cosmic ray data sample.

A prototype of the chamber was used to study the resolution with different gases. With dimethyl ether, 40 μm spatial resolution was achieved at one atmosphere absolute. This result is tantalising; even better resolution should be attainable at higher pressures. Care must be taken, however, in the choice of chamber components if one is to use DME. Its effects on several materials are adverse. Studies were made to enhance the lifetime of a test chamber. Both frequent gas circulation and the addition of small amounts of water proved beneficial.

13. Acknowledgements

We would like to thank B. Collins, C. Hudspeth, and L. Salgado for their help with the construction of the chamber.

References

1. P. Baringer *et al.*, NIM A 254 (1987) 542.

2. W.W. Ash *et al.*, NIM A 261 (1987) 399.

3. W.T. Ford *et al.*, NIM A 255 (1987) 486.

4. Mylar is a registered trademark of E.I. Dupont de Nemours & Co. (Inc.), Industrial Films Division, Wilmington, Delaware 19898.

5. Throughout this paper, we use argon-ethane to denote the mixture, argon (50%) ethane (50%), supplied premixed by Matheson Gas Products, Inc., 30-T Seaview Dr., Secaucus, NJ 07094. For some tests, we have added to the argon-ethane small admixtures ($< 1\%$) of water and alcohols. These are referred to explicitly.

6. The pressure vessel was made by the Advanced Composite Product and and Technology Company, 7415 Mount Joy Drive, Huntington Beach, CA 92648.

7. Kapton is a registered trademark of E.I. Dupont de Nemours & Co. (Inc.), Industrial Films Division, Wilmington, Delaware 19898.

8. The straws were manufactured by the Euclid Spiral Paper Tube Corp., 339 Mill Street, P.O. Box 458, Apple Creek, OH 44094. Sheldahl, P.O. Box 170, Northfield, MN 55057 supplied the aluminized Mylar.

9. Delrin is a registered trademark of E.I. Dupont de Nemours & Co. (Inc.). We have used virgin Delrin 500.

10. Eccobond 66C Catalyst 9 epoxy made by Emerson and Cuming, Inc., Canton, MA 02021.

11. The hole coordinates were measured using a Validator 150 machine made by Brown and Sharpe Mfg. Co., Precision Park, North Kingstown, RI 02852.

12. We used Stycast 2850 FT/24 LV epoxy made by Emerson and Cuming, Canton, MA 02021.

13. The ^{55}Fe source was custom-made by Isotope Products Lab., 1800 N. Keystone St., Burbank, CA 91504.

14. The black Viton O-rings were obtained from Bay Seal Co., 1550 West Winton, Hayward CA 94545.

15. Datametrics, 340 Fordham Road, Wilmington, MA 01887, supplied the gas system hardware.

16. Brooks Instrument Div., Emerson Electric Co., 409 W. Vine St., Hatfield, PA 19440.

17. Analog Devices Inc., 2-T Technology Way, Norwood, MA 02062.

18. Bertan Associates Inc., 121-T New South Road, Hicksville, NY 11801.

19. The cables (type 9252) are rated for 5.3 kV and were obtained from Control Master Products, 1028 Shary Circle, Concord CA 94520.

20. Avantek Inc., 4401-T Great America Pkwy., Santa Clara, CA 95054.

21. LeCroy Research Systems Corp., 700-T S. Main St., Spring Valley, NY 10977.

22. E.L. Cisneros *et al.*, IEEE Trans. Nuc. Science NS-24 1 (1977) 413.

23. Power Designs Inc., 1700-T Shames Dr., Westbury, NJ 11590.

24. M. Breidenbach *et al.*, IEEE Trans Nuc. Science NS-25 1 (1978) 706.

25. The Mark III coordinate system is defined as follows: x is the horizontal axis pointing toward the center of the SPEAR ring; y, the vertical axis; and z, the axis along the beam.

26. D. Pitman *et al.*, Nucl. Instr. and Meth. A265 (1988) 85.

27. G-10 is a NEMA standard for a non-brominated woven fibreglass-epoxy laminate.

28. Stesalit, a non-woven fibreglass matting embedded in epoxy resin, is a registered trademark of Stesalit AG, Zullwil, SO., Switzerland.

29. Celanese X made by Celanese Corp., 1211-T Avenue of the Americas, New York, N.Y. 10036.

30. See for example the Proceedings of the Workshop on Radiation Damage to Wire Chambers, LBL, Berkeley, 1986.

31. J.J.Thaler *et al.*, IEEE Transactions on Nuclear Science NS-30 1 (1983) 236.

Figure Captions

1. A cutaway drawing of the vertex chamber showing axial and stereo straws, the beampipe, endplates and the pressure shell.

2. A cross-section of the vertex chamber showing the arrangement of the straws.

3. A drawing showing a detail of the straw mounted in the endplate, with its feedthrough assembly.

4. A schematic of the circuit for one high voltage/readout board.

5. The gain of the amplifier as a function of input frequency, shown for both the 2-stage and 3-stage amplifier configurations.

6. a) Input and b) output pulses, showing a risetime of 1.5 ns for the amplifier. The horizontal axis is 500 ps/division.

7. The noise counting rate of the amplifier/discriminator as a function of the discriminator threshold setting.

8. The results of a fit to a cosmic ray track. The centers of the circles represent the locations of sense wires which gave signals; the radius of a circle indicates the calculated drift distance for that straw.

9. Residuals for all cells, selecting tracks which pass within 2.54 cm of the center of the chamber. The fitted resolution is 49 μm.

10. The spatial resolution as a function of the radial distance of the track from the wire.

11. The single tube spatial resolution for the prototype chamber using a) argon-ethane at various pressures, and b) dimethyl ether at 1 atmosphere absolute.

12. The effects of various pressurized gases on aluminized Mylar; a) the relative change in weight and b) the relative change in length of the samples. The measurement errors in a) are smaller than the point sizes.

13. The effects of DME and argon-ethane with 0.5% ethanol on some commonly used drift chamber materials. The relative change in weight of the samples is shown.

14. Typical trigger element with accompanying logic diagram for cells contained a) in layers 2, 3, and 4 and b) in layers 1, 3, and 4. The outer axial layers are treated analogously. c) An inner axial layer element combined with the three possible elements from the outer axial layers.

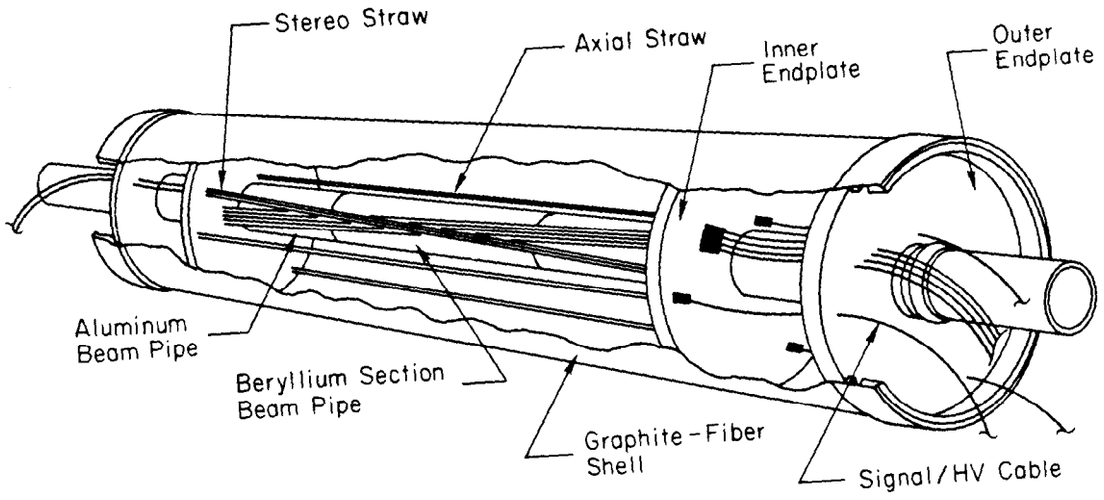
Stereo Straw
Axial Straw
Inner Endplate
Outer Endplate
Aluminum Beam Pipe
Beryllium Section Beam Pipe
Graphite-Fiber Shell
Signal/HV Cable
4-88
6011B5

Fig. 1

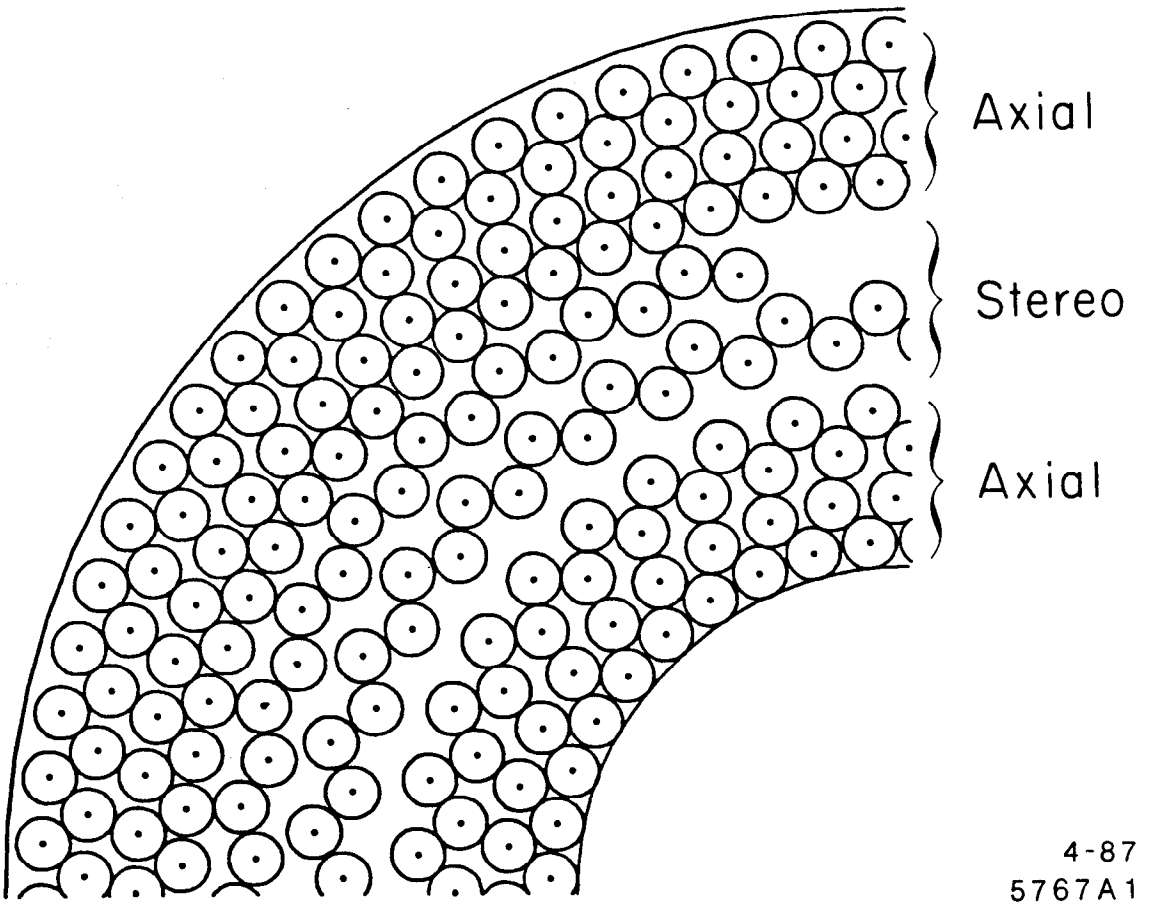

Fig. 2

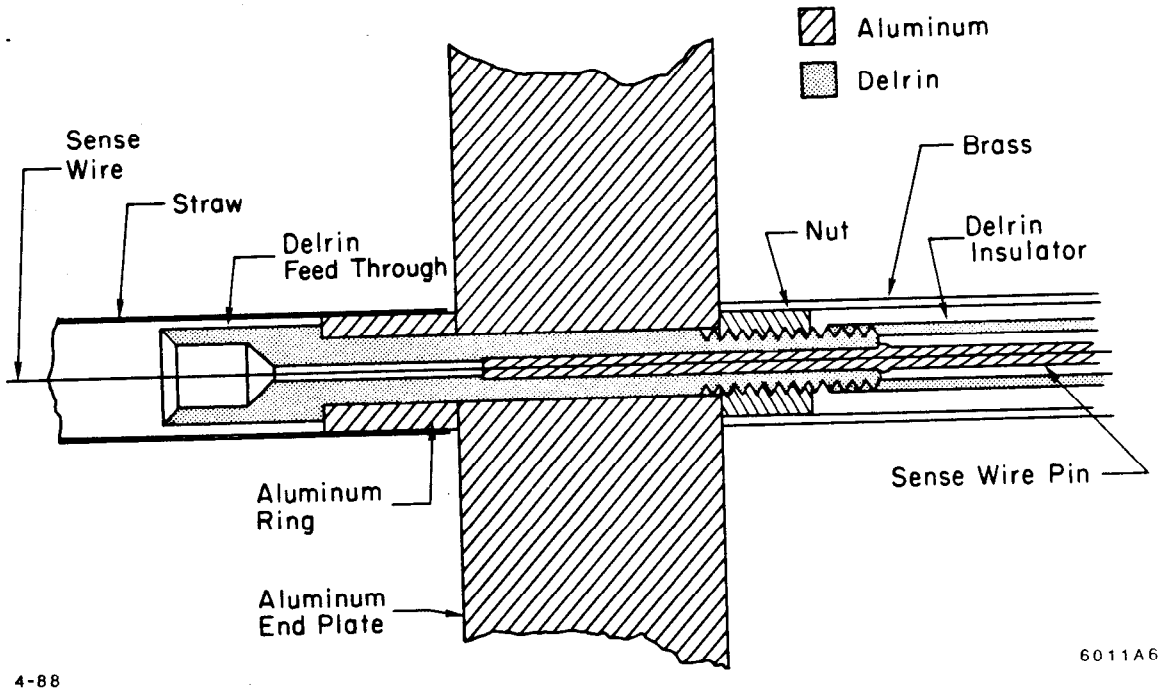
Aluminum
Delrin
Sense Wire
Straw
Delrin Feed Through
Brass
Nut
Delrin Insulator
Aluminum Ring
Aluminum End Plate
Sense Wire Pin
4-88
6011A6

Fig. 3

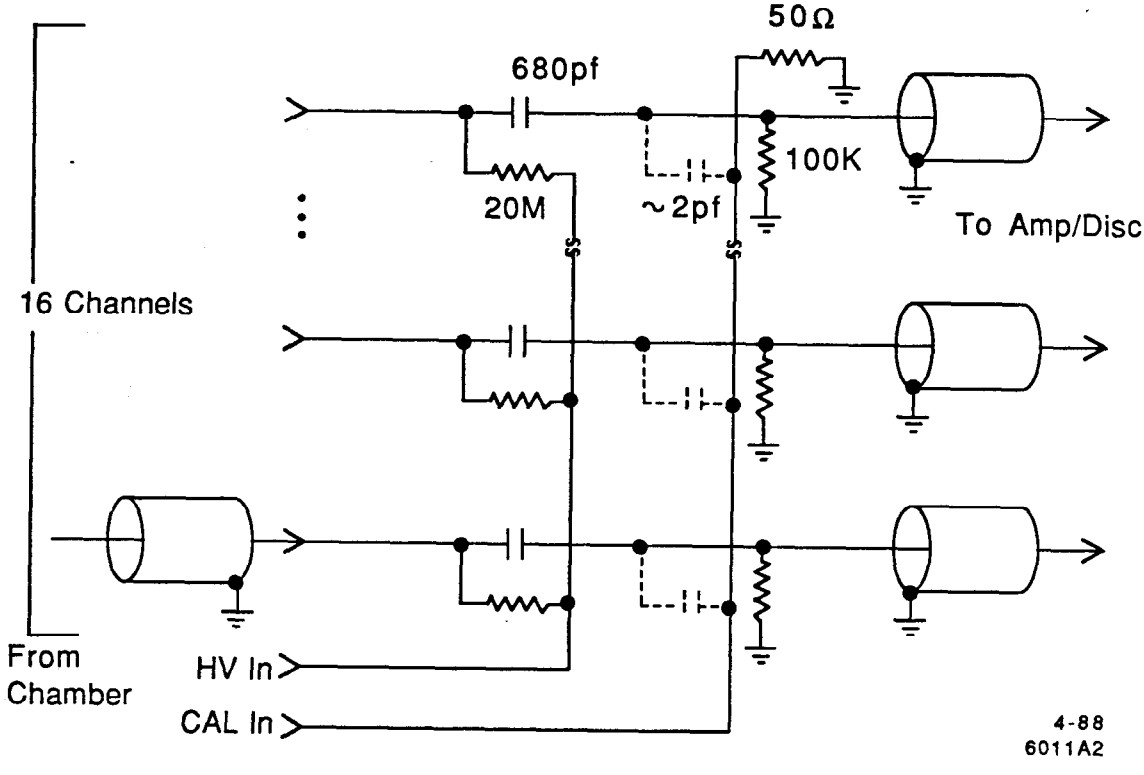
50Ω
680pf
100K
20M
~2pf
To Amp/Disc
16 Channels
From
Chamber
HV In
CAL In
4-88
6011A2

Fig. 4

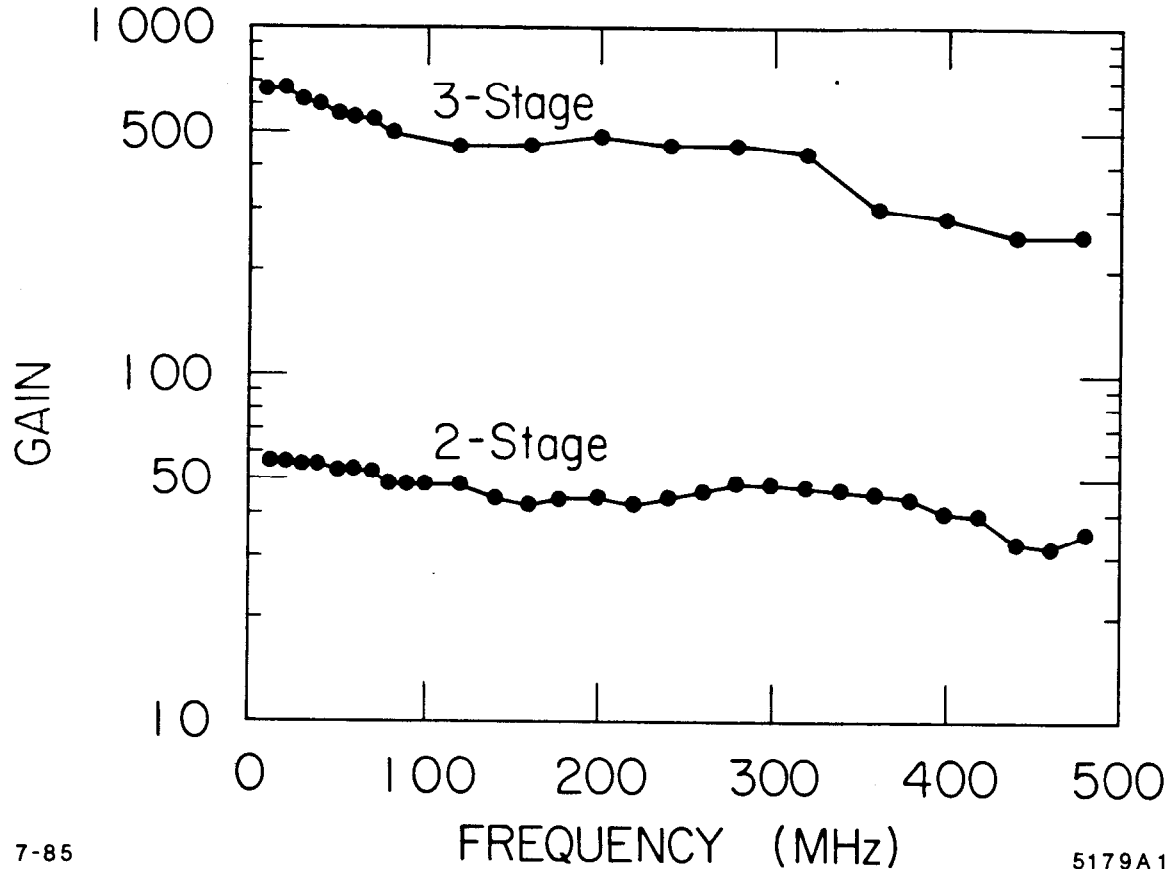
1000
500
100
50
10
GAIN
3-Stage
2-Stage
0
100
200
300
400
500
FREQUENCY (MHz)
7-85
5179A1

Fig. 5

(a)

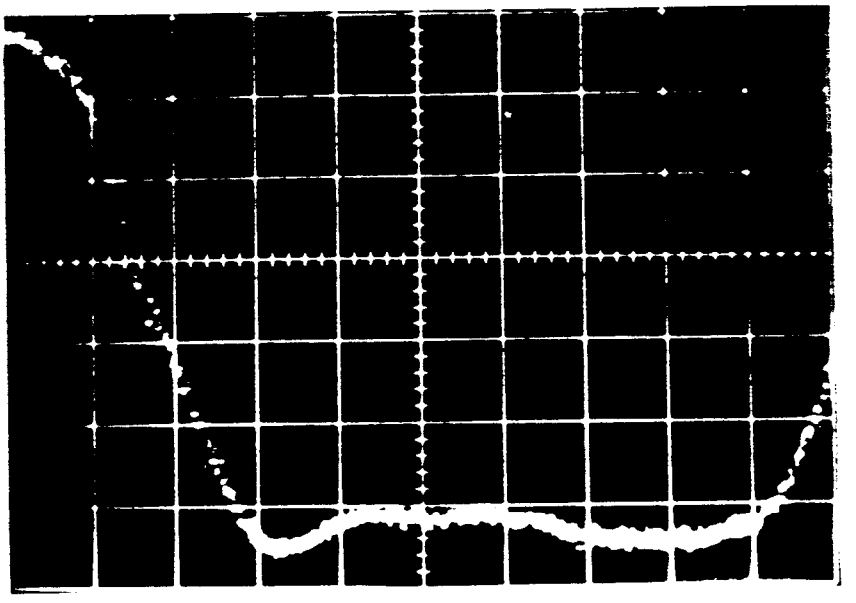

(b)

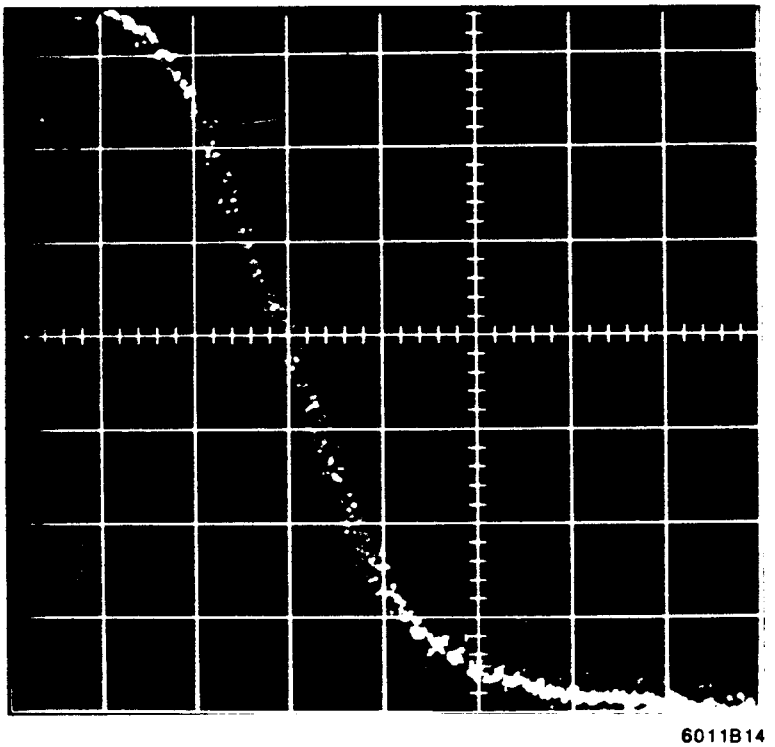

8-88

6011B14

Fig. 6

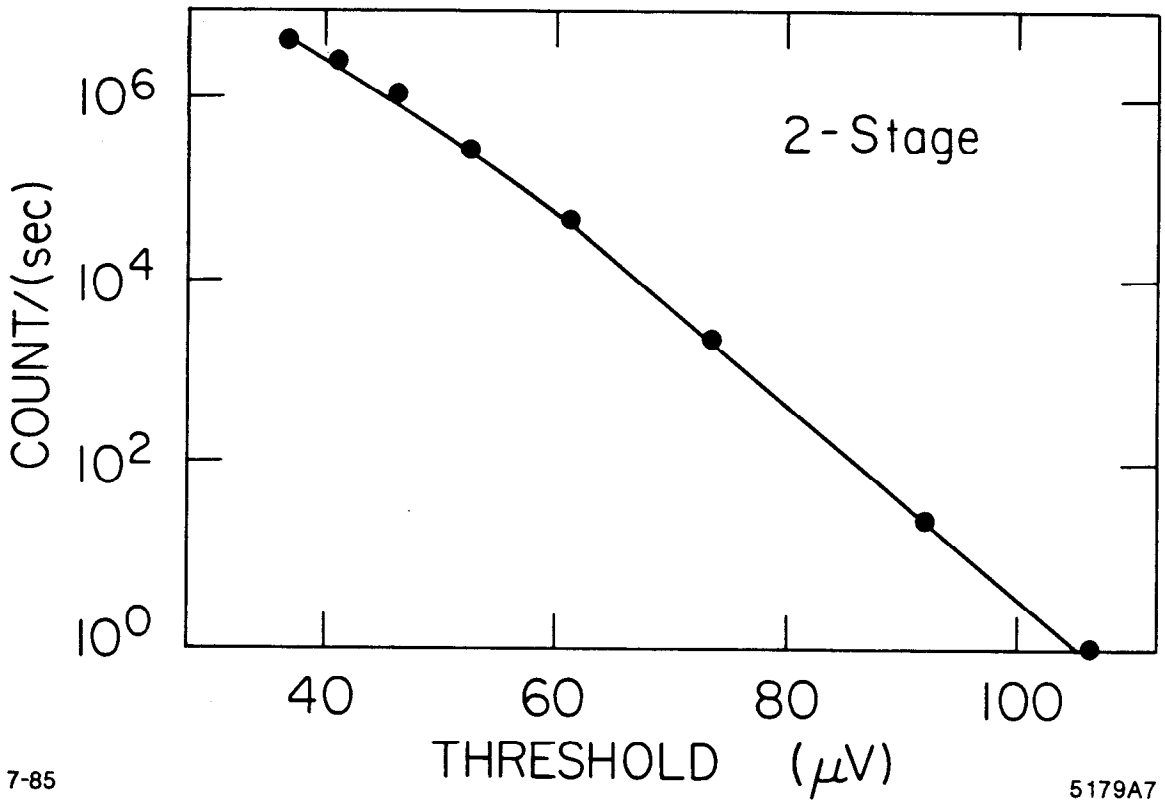
2-Stage
COUNT/(sec)
10^6
10^4
10^2
10^0
40
60
80
100
THRESHOLD (μV)
7-85
5179A7

Fig. 7

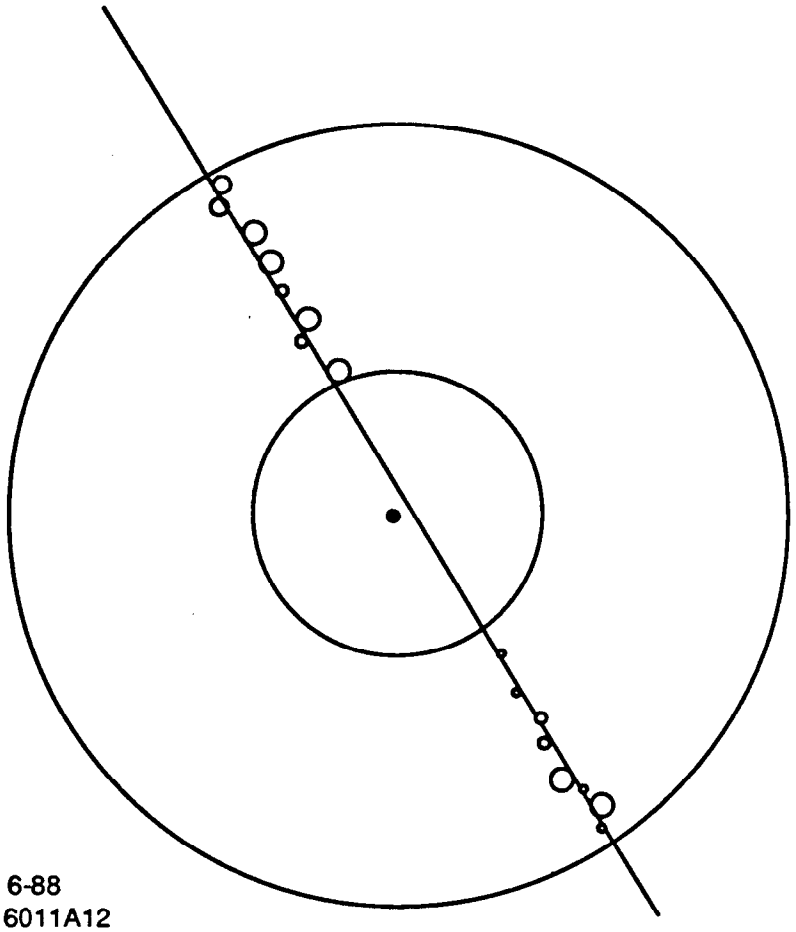

6-88
6011A12

Fig. 8

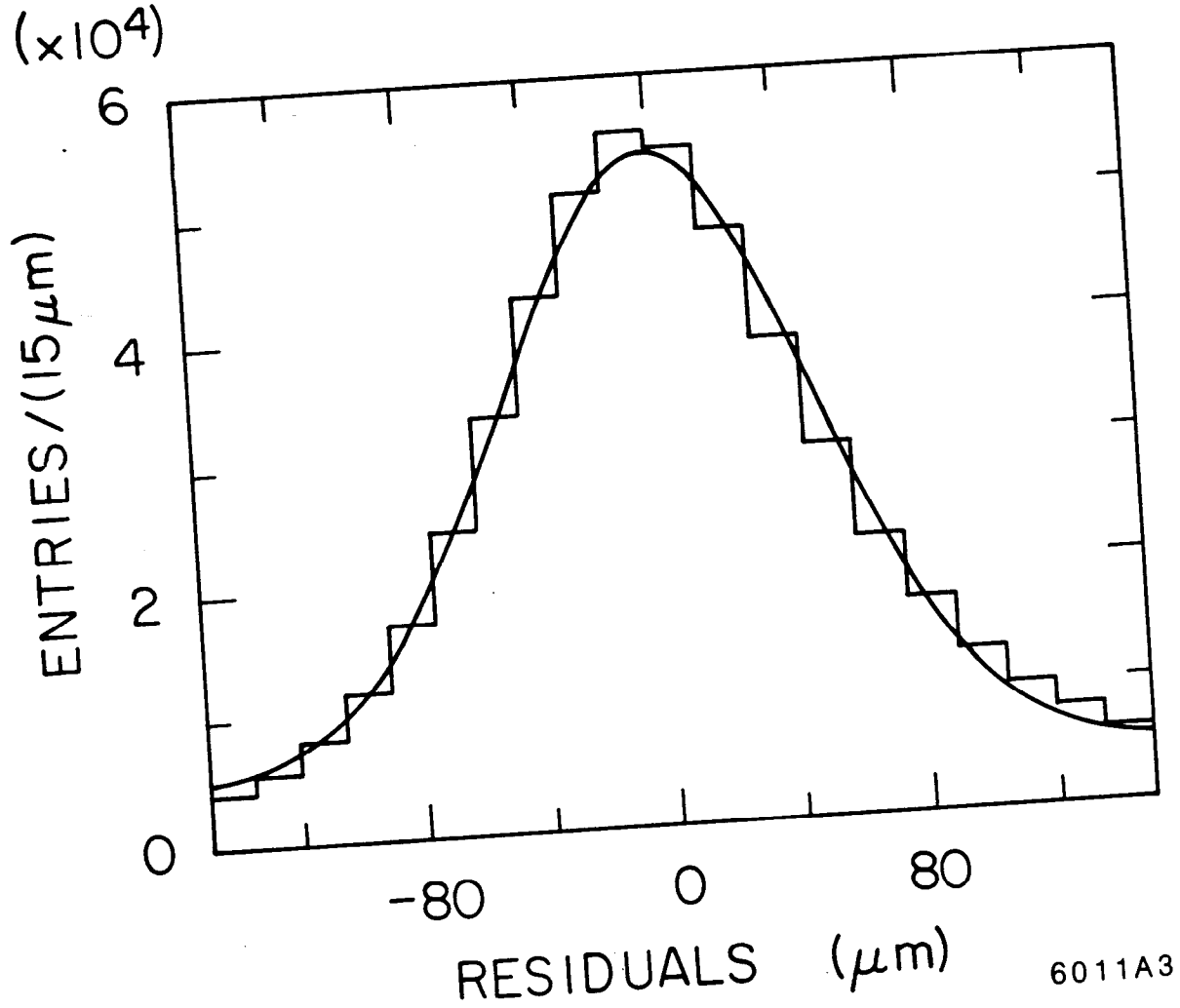

4-88

Fig. 9

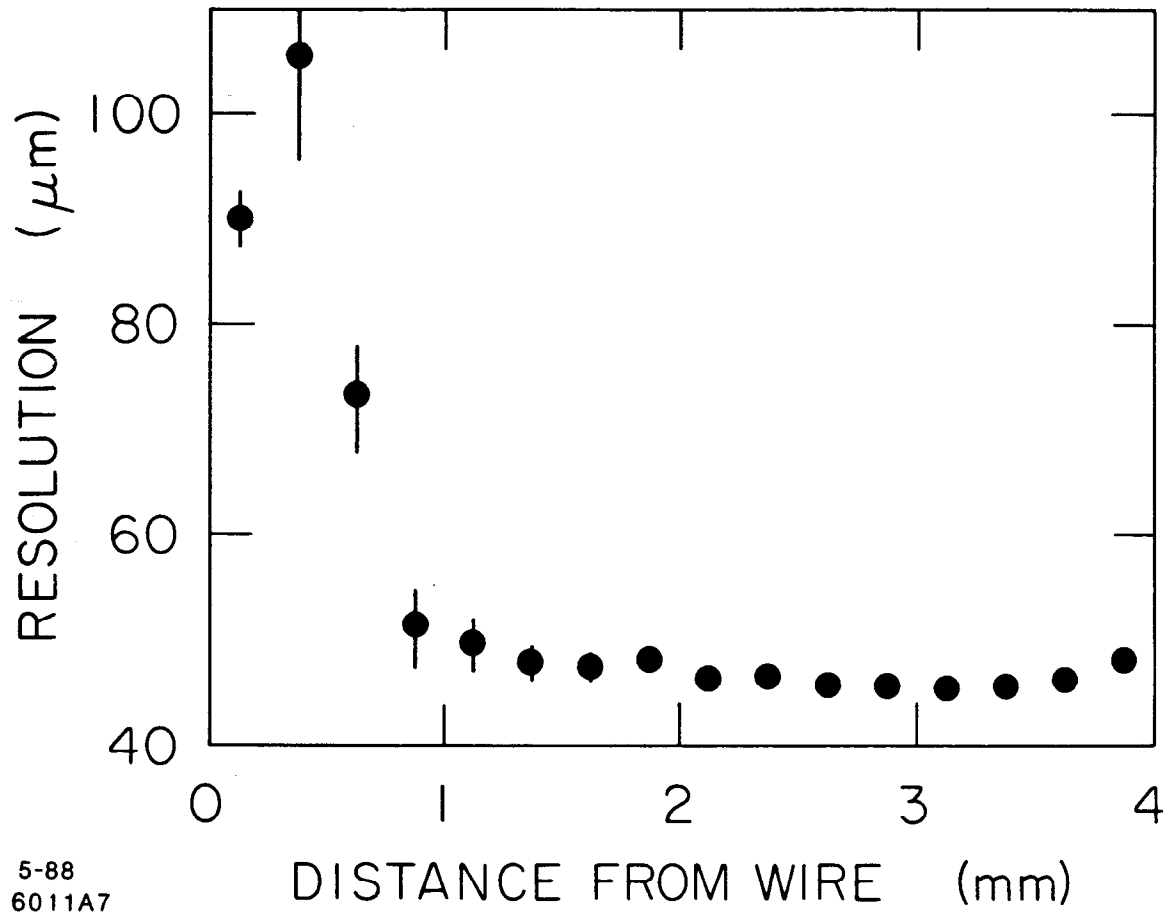
RESOLUTION (μm)
100
80
60
40
0
1
2
3
4
DISTANCE FROM WIRE (mm)
5-88
6011A7

Fig. 10

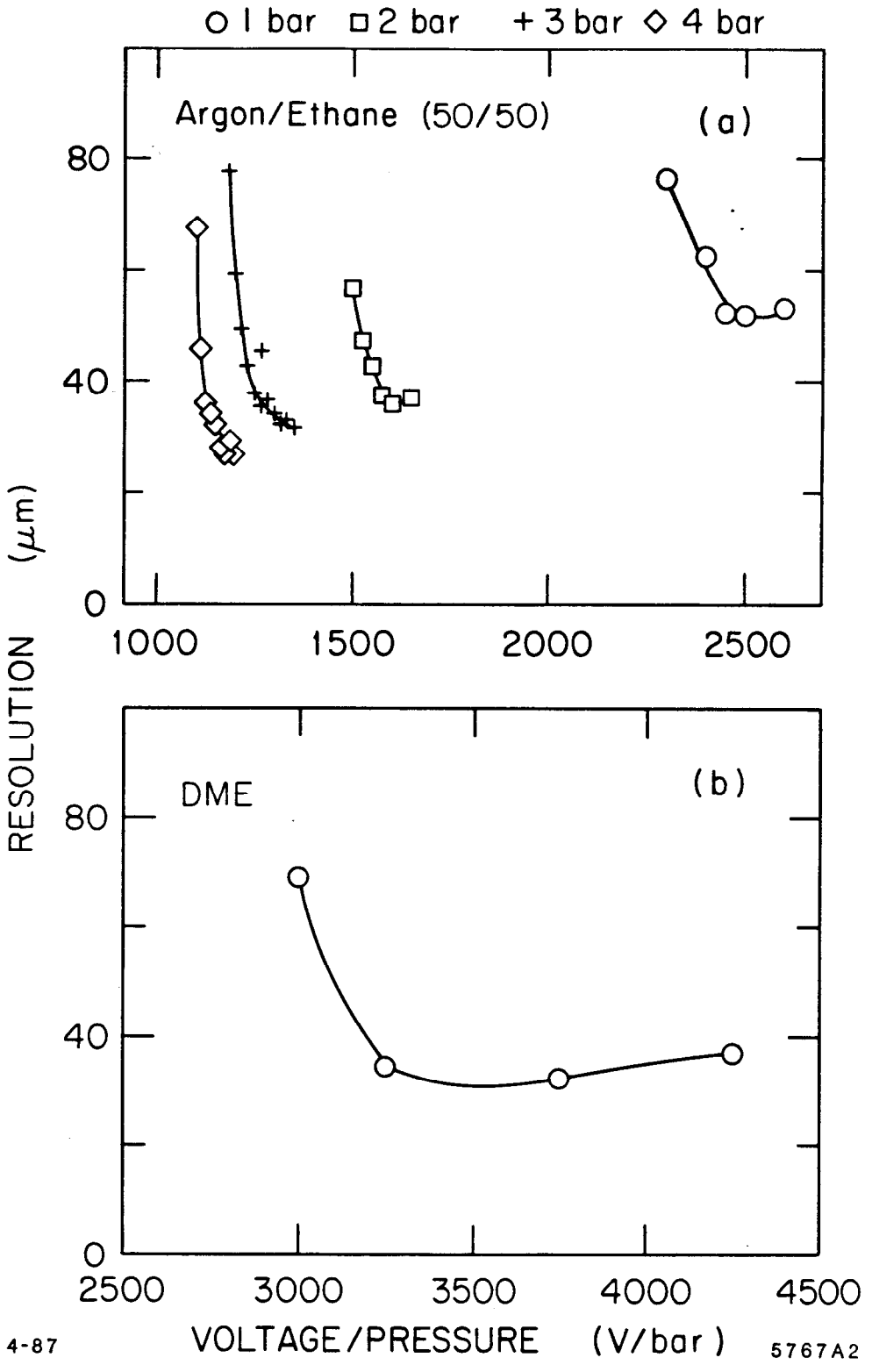
○ 1 bar □ 2 bar + 3 bar ◇ 4 bar
Argon/Ethane (50/50)
(a)
80
40
0
1000
1500
2000
2500
RESOLUTION (μm)
DME
(b)
80
40
0
2500
3000
3500
4000
4500
4-87
VOLTAGE/PRESSURE (V/bar)
5767A2

Fig. 11

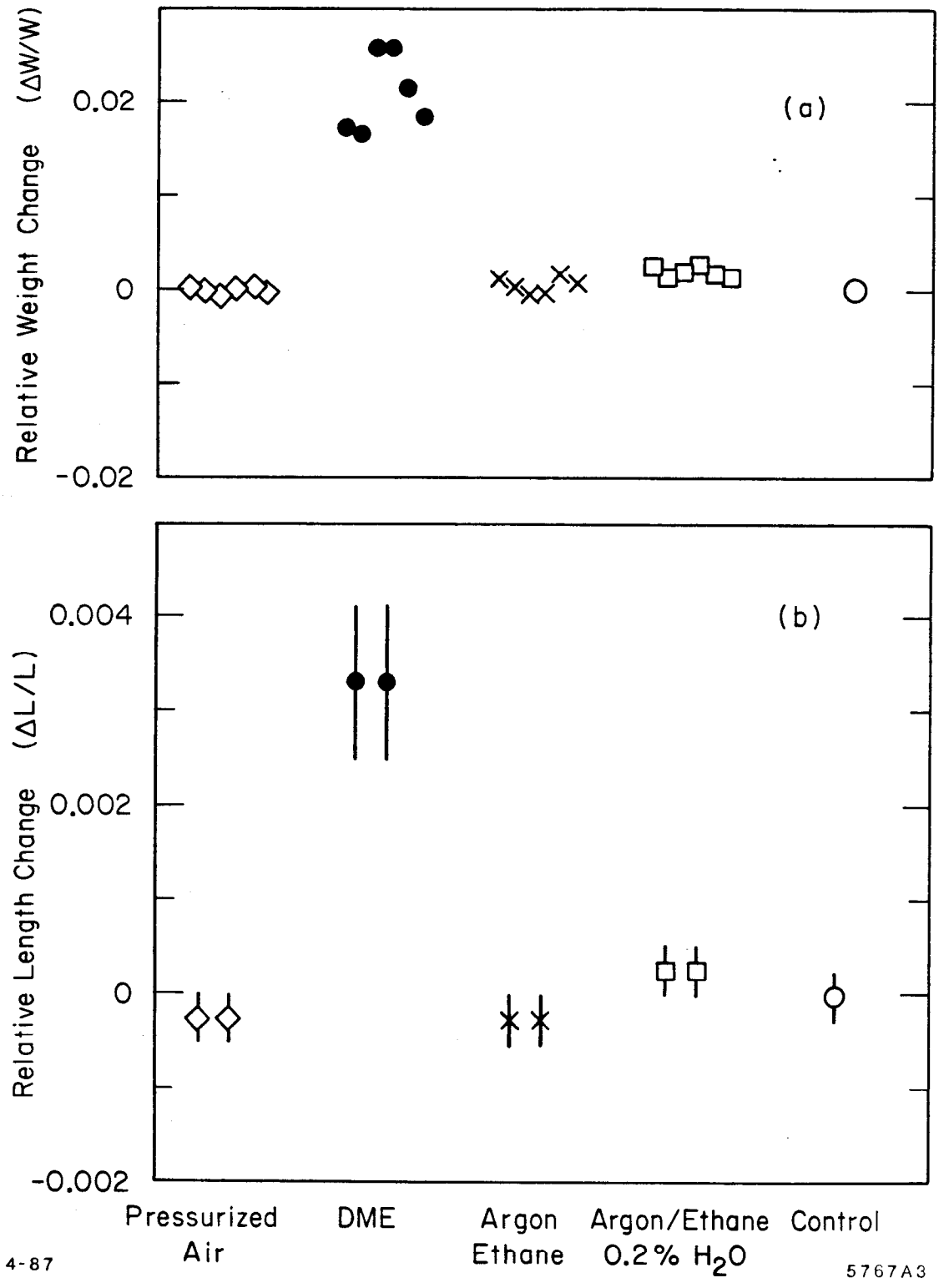
Relative Weight Change (ΔW/W)
0.02
0
-0.02
(a)
Relative Length Change (ΔL/L)
0.004
0.002
0
-0.002
(b)
Pressurized Air
DME
Argon Ethane
Argon/Ethane 0.2% H2O
Control
4-87
5767A3

Fig. 12

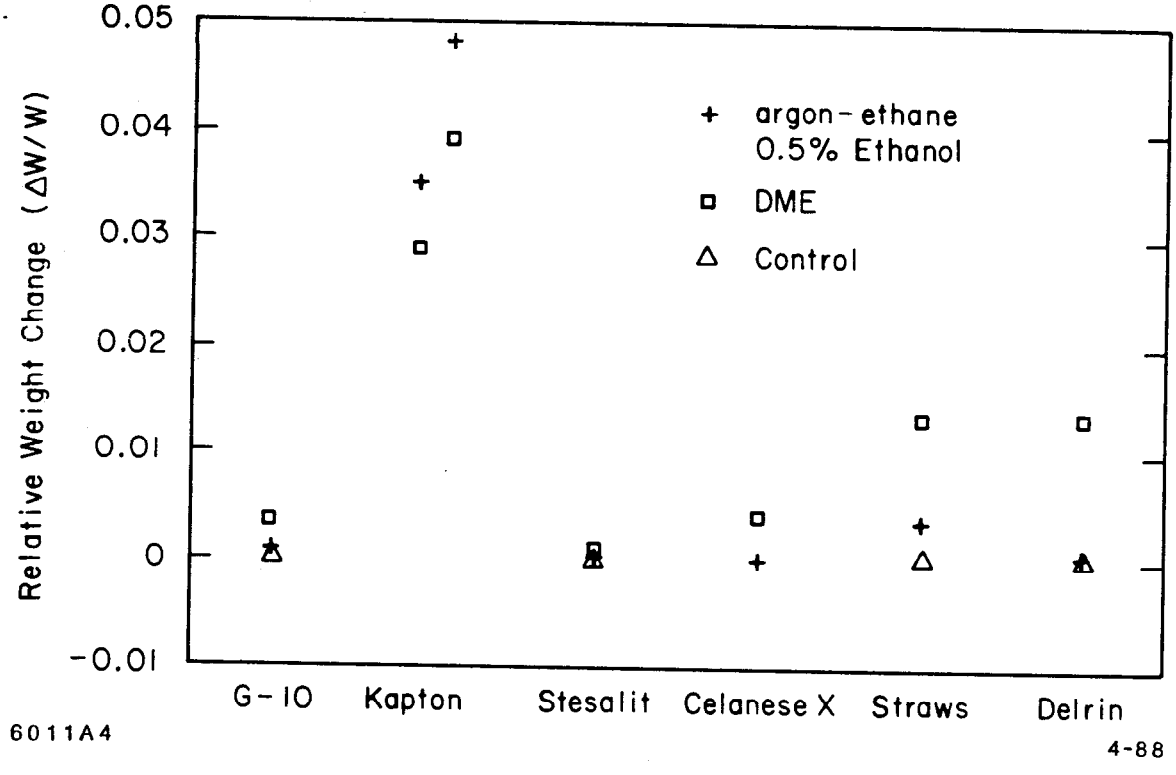
0.05
0.04
0.03
0.02
0.01
0
-0.01
Relative Weight Change (ΔW/W)
argon-ethane
0.5% Ethanol
DME
Control
G-10
Kapton
Stesalit
Celanese X
Straws
Delrin
6011A4
4-88

Fig. 13

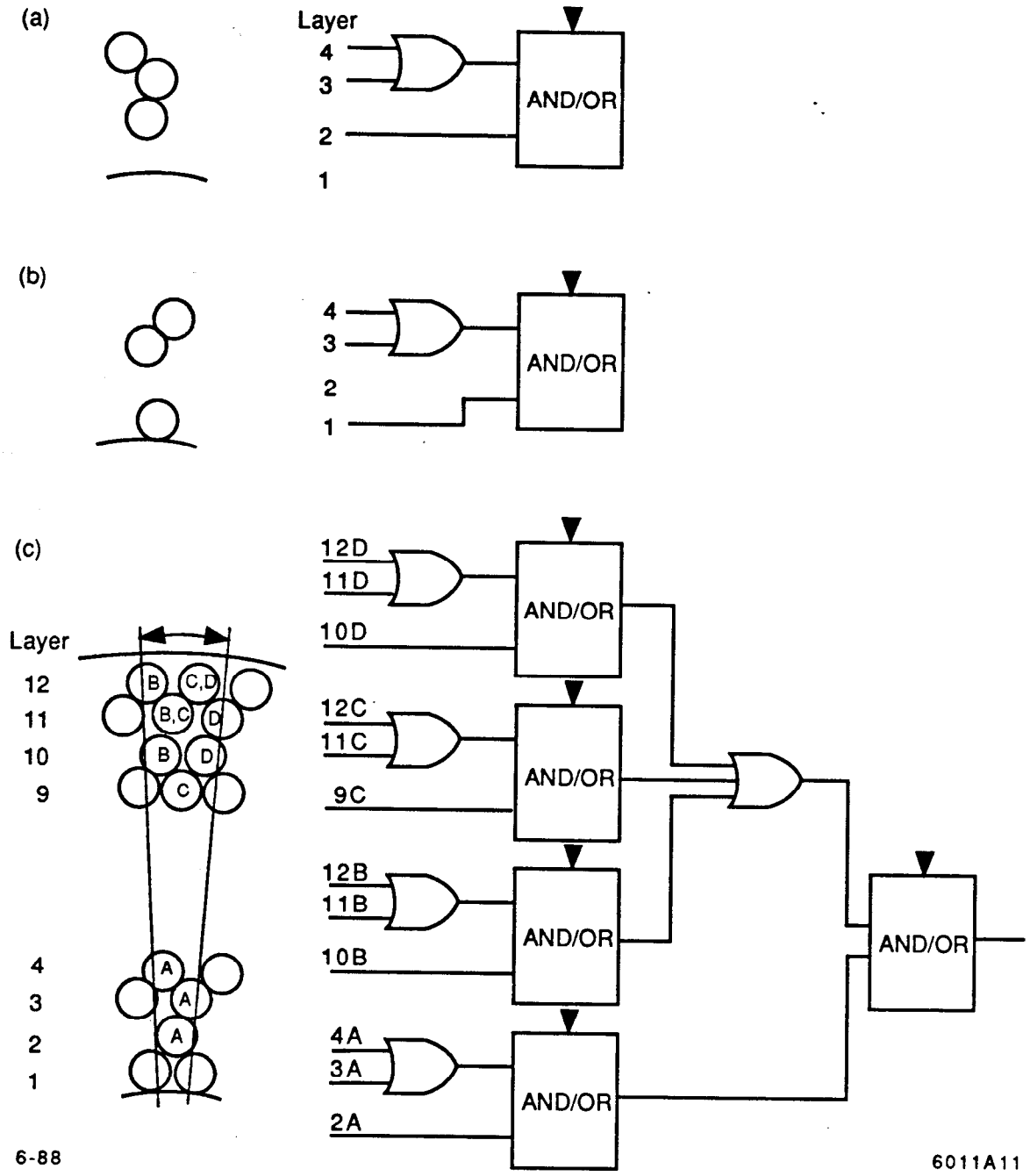
(a)
Layer
4
3
2
1
AND/OR
(b)
4
3
2
1
AND/OR
(c)
Layer
12
11
10
9
4
3
2
1
B
C,D
B,C
D
B
D
C
A
A
A
12D
11D
10D
12C
11C
9C
12B
11B
10B
4A
3A
2A
AND/OR
AND/OR
AND/OR
AND/OR
AND/OR
6-88
6011A11

Fig. 14